J Sci Comput (2013) 54:492–512
DOI 10.1007/s10915-012-9629-0

Efficient Rearrangement Algorithms for Shape Optimization on Elliptic Eigenvalue Problems

Chiu-Yen Kao · Shu Su

Received: 17 January 2012 / Revised: 29 May 2012 / Accepted: 6 July 2012 / Published online: 24 July 2012

Abstract In this paper, several efficient rearrangement algorithms are proposed to find the optimal shape and topology for elliptic eigenvalue problems with inhomogeneous structures. The goal is to solve minimization and maximization of the k-th eigenvalue and maximization of spectrum ratios of the second order elliptic differential operator. Physically, these problems are motivated by the frequency control based on density distribution of vibrating membranes. The methods proposed are based on Rayleigh quotient formulation of eigenvalues and rearrangement algorithms which can handle topology changes automatically. Due to the efficient rearrangement strategy, the new proposed methods are more efficient than classical level set approaches based on shape and/or topological derivatives. Numerous numerical examples are provided to demonstrate the robustness and efficiency of new approach.

Keywords Minimal eigenvalue · Maximal eigenvalue · Maximal ratio of eigenvalues · Elliptic operator · Shape optimization · Rearrangement algorithm · Rayleigh quotient

1 Introduction

Shape and topology optimization involving eigenvalues arise naturally in many different fields, such as mechanical vibrations, electromagnetic cavities, photonic crystals, and population dynamics. Since it is usually difficult to find the closed-form solution for most shape and topology optimization problems, numerical approaches become necessary and

C.-Y. Kao (✉)
Department of Mathematics, The Ohio State University Columbus, Columbus, OH 43210, USA
e-mail: kao@math.ohio-state.edu

C.-Y. Kao
Department of Mathematics and Computer Science, Claremont McKenna College, Claremont, CA 91711, USA

S. Su
American Electric Power, Columbus, OH 43215, USA
e-mail: ssu@aep.com

can sometimes guide analytic approaches. Common numerical approach is to start with an initial guess for a shape and then gradually evolve it, until it morphs into an optimal shape. Since the initial guess may not have the same topology as the optimal shape, it is important to develop numerical techniques to handle topology changes.

The most popular method to evolve the shape is based on the shape derivative [18, 23] which characterizes the sensitivity of a smooth variation of the boundary. However, this approach suffers from two main drawbacks: the requirement of a smooth parametrization of the boundary and the difficulty to accommodate topological changes. To overcome this limitation, homogenization approaches have been introduced [1, 4]. However, these methods are mainly restricted to linear elasticity and particular objective functions. In order to have broader applications, developing numerical techniques which can handle both shape and topology changes becomes essential for shape and topology optimization problems.

The level set method introduced in [20] has been well known for its ability to handle topology changes, such as breaking one component into several, merging several components into one and forming sharp corners. Therefore it has been used naturally to study shape optimization problems. Instead of using the physically driven velocity, the level set method typically moves the surfaces by the gradient flow of an objective energy functional. The approaches based on shape derivatives [5, 13, 15, 19, 22] and/or topological derivatives [2, 6] have been demonstrated to successfully change the shape flexibly and find the optimal shapes. These approaches have been applied to the study of extremum problems of eigenvalue of inhomogeneous structure, including identification of composite membranes with extremum eigenvalue [11, 19, 26], design of composite materials with desired spectrum gap or maximal spectrum gap [15], finding optical devices which have high quality factor (low loss of energy) [16], and principle eigenvalue optimization in population biology [14]. Since both shape and topological derivatives are based on local perturbation of shape, without other special treatments, the algorithms usually require many iterations to converge. In [10], a multi-level continuation technique was proposed to accelerate the speed of the algorithm for identification of composite membranes with extremum eigenvalue. Another type of efficient approaches for minimizing the first eigenvalue is the binary update based on finding the threshold in principle eigenfunction [7, 14, 24].

In this work, the focus is placed on the study of structural vibration frequency control of acoustic drum problems based on changing the density distribution. We proposed several rearrangement algorithms to find the optimal density distribution with prescribed mass constraint so that the k-th frequency and ratio of frequencies of the resulting membrane is extremized. Most of previous results are for the first eigenmode with Dirichlet boundary condition. Here we study general higher eigenmodes with different boundary conditions. The approaches are based on Rayleigh quotient formulation of eigenvalues and rearrangement algorithms which not only handle topological changes automatically but also converges efficiently. Additionally, the number of iteration for convergence does not really increase when the mesh is refined. We further introduce fully rearrangement and partial rearrangement algorithms to alter the density in the global and local ways. The fully rearrangement approach looks for the optimal rearrangement at each iteration while the partial rearrangement approach takes moderate changes to generate satisfactory result. The approaches based on shape derivatives and topological derivatives can be considered as examples of partial rearrangements.

The paper is organized as follows: in Sect. 2, the mathematical formulation of the eigenvalue problem for inhomogeneous vibrating membranes is introduced and some of theoretical results are reviewed. In Sect. 3, we present new approaches based on Rayleigh quotient formulation of eigenvalues and several different rearrangement algorithms. In Sect. 4, we

discuss the numerical implementation. To demonstrate the capability and efficiency of the numerical approach, we apply it to solve many different elliptic eigenvalue extremum problems in inhomogeneous medium.

2 Inhomogeneous Vibrating Membranes

2.1 Mathematical Formulation

Here we consider a vibrating membrane with a fixed bounded domain $D \subset \Re^n$, and a variable density $\rho(x)$. The displacement from rest, u, of a membrane satisfies

$$-\Delta u(x) = \lambda \rho(x) u(x), \quad \text{for } x \in D, \tag{1}$$

where λ is the eigenvalue of the membrane and it is related to the square of vibrating frequencies. This equation arises from the reduction of wave equation. Depending on the boundary condition

$$\frac{\partial u}{\partial n} + \beta u = 0, \quad \text{for } x \in \partial D, \tag{2}$$

where β is a constant parameter, the spectrum of eigenvalues has different properties. For clamped membranes, $u(x) = 0$ for $x \in \partial D$ (Dirichlet boundary condition, i.e. $\beta = \infty$), there exists a sequence of such eigenvalues

$$0 < \lambda_1(\rho) < \lambda_2(\rho) \leq \lambda_3(\rho) \leq \cdots \leq \lambda_k(\rho) \leq \lambda_{k+1}(\rho) \leq \cdots \uparrow \infty,$$

where each $\lambda_k(\rho, D)$ is counted with its multiplicity. However, for boundary which can move freely, $\partial u/\partial n = 0$ for $x \in \partial D$ (Neumann boundary condition, i.e. $\beta = 0$), the spectrum consists of eigenvalues

$$0 = \lambda_0(\rho) \leq \lambda_1(\rho) \leq \lambda_2(\rho) \leq \cdots \leq \lambda_k(\rho) \leq \lambda_{k+1}(\rho) \leq \cdots \uparrow \infty.$$

Different boundary conditions and density configurations give different eigenvalue distributions. Under the assumption of fixed weight and boundness, i.e.

$$\int_D \rho(x)dx = W \quad \text{and} \quad \rho_1 \leq \rho(x) \leq \rho_2, \tag{3}$$

where ρ_1, ρ_2, and W are prescribed positive constants, we want to find the optimal density distribution that solves the following extremal eigenvalue problems:

$$\min_{\rho(x)} \lambda_k, \quad \max_{\rho(x)} \lambda_k, \quad \text{or} \quad \max_{\rho(x)} \lambda_{k_2}/\lambda_{k_1}, \tag{4}$$

for a given fixed k or both k_1 and k_2.

2.2 Some Theoretical Results

The optimal density distribution for minimization and maximization of a specific eigenvalue λ_k in one dimension, which describes the vibration of ropes, satisfies

$$-u''(x) = \lambda \rho(x) u(x),$$

in the domain $x \in (0, 1)$, with the zero Dirichlet boundary conditions, i.e.

$$u(0) = u(1) = 0,$$

was found by Krein [17]. He proved that the optimal density distributions with the constraint $\int_0^1 \rho(x)dx = W = \rho_1\gamma + \rho_2(1-\gamma)$ which minimize (maximize) the k-th eigenvalue are $\check{\rho}_k^\gamma(\hat{\rho}_k^\gamma)$:

$$\check{\rho}_k^\gamma(x) = \begin{cases} \rho_2 & \text{if } x \in (m_k^j - \frac{1-\gamma}{2k}, m_k^j + \frac{1-\gamma}{2k}),\ j = 1, 2, \ldots, k, \\ \rho_1 & \text{otherwise,} \end{cases}$$

$$\hat{\rho}_k^\gamma(x) = \begin{cases} \rho_1 & \text{if } x \in (m_k^j - \frac{\gamma}{2k}, m_k^j + \frac{\gamma}{2k}),\ j = 1, 2, \ldots, k, \\ \rho_2 & \text{otherwise,} \end{cases}$$

where $m_k^j = (2j-1)/2k$ is the midpoint of the interval $((j-1)/k, j/k)$. The interesting feature of these solutions is the "bang-bang" structure of the density, i.e. the density is a piecewise constant function. Later Cox and McLaughlin [8] studied the membrane vibration problem (1) with Dirichlet boundary condition. They addressed the existence of the extremizers and found that the extremizers also have "bang bang" structure. Additionally, the interface between two different densities can be characterized by a level set curve of the eigenfunction. For example, let $\tilde{\rho}$ be a minimizer (maximizer) of $\lambda_1(\rho)$ and u_1 be the associated eigenfunction, then there exists a constant u_T such that, for each $x \in D$,

$$\begin{cases} \tilde{\rho}(x) = \rho_2(\rho_1) & \text{if } u_1(x) > u_T, \\ \tilde{\rho}(x) = \rho_1(\rho_2) & \text{if } u_1(x) < u_T, \end{cases}$$

and

$$\tilde{\rho}(\Omega) = \rho_1\chi_{D\setminus\Omega} + \rho_2\chi_\Omega(\rho_2\chi_{D\setminus\Omega} + \rho_1\chi_\Omega),$$

where Ω is the level set $\Omega = \{x \in D | u_1(x) \geq u_T\}$. We remark here that the maximizer is unique while the uniqueness of the minimizer is not guaranteed. In particular, a dumbbell shaped domain under certain setting will give at least two minimizers and the complement of each optimal set is contained in one of the lobes [12].

3 Numerical Methods

The numerical approach for minimizing (maximizing) eigenvalue problems consists of two parts: (1) forward solver: given a density distribution ρ, find its corresponding eigenvalues λ_k and eigenfunctions u_k, and (2) inverse solver: given eigenvalues and eigenfunctions, determine the new distribution of ρ such that the objective function decreases (increases).

3.1 Finite Element Forward Solver

In order to do computation on complicated domains with a given density function ρ, we use finite element method (FEM) to solve (1) and (2). We assume that ρ is constant in each element. First, the eigenfunction is expanded in the FEM basis ($u = \sum_{i=1}^{i=n} U_i^h \xi_i$ where ξ_i are basis functions), and then plugging into the equation which was multiplied by a test basis function, and then integrated on the domain D. This process yields a generalized eigenvalue equation which can be solved by the Arnoldi algorithm. It can be implemented easily by using the Matlab Partial Differential Equation Toolbox subrountine "pdeeig".

3.2 Fully Sorting Algorithm for Minimization of λ_k

We start with finding the optimal density configuration ρ which minimizes the eigenvalue λ_k of (1) with the boundary condition (2) and the constraint (3). The main tool in this endeavor is the variational characterization of eigenvalues as the Poincaré principle or Courant-Fischer formulae [12, 21]. Define the Rayleigh quotient of the second order elliptic operator L as

$$R_L[v] := \frac{\int_D |\nabla v|^2 dx + \beta \int_{\partial D} v^2(x) dx}{\int_D \rho(x) v(x)^2 dx}.$$

Then, we have

$$\lambda_k^D = \min_{\substack{v \in H_0^1(D) \\ v \text{ orthogonal to } u_1, u_2, \ldots, u_{k-1}}} R_L(v),$$

where u_k is the k-th eigenfunction for Dirichlet boundary condition and

$$\lambda_k^{N(R)} = \min_{\substack{v \in H^1(D) \\ v \text{ orthogonal to } u_1, u_2, \ldots, u_{k-1}}} R_L(v),$$

for Neumann (Robin) boundary conditions. Suppose the initial density is

$$\rho = \begin{cases} \rho_1 & \text{for } x \in D/\Omega, \\ \rho_2 & \text{for } x \in \Omega, \end{cases}$$

where $\Omega \subset D$ is a bounded subset inside D. The gradient descend approach for the Dirichlet problem [19] lies on the computation of the gradient of a simple k-th eigenvalue λ_k

$$\delta \lambda_k = -\frac{\lambda_k \int_D \delta\rho \cdot u_k^2 dx}{\int_D \rho u_k^2 dx}. \tag{5}$$

If we choose $\delta\rho = a u_k^2$ where a is a positive constant, a descent direction is guaranteed because $\delta\lambda_k < 0$. This descent direction implies that the eigenvalue λ_k decreases as the density function $\rho(x)$ increases quadratically in u. However, this approach cannot allow piecewise distributions of the density.

Instead, an iterative fully sorting algorithm can be used so that the constraint on the density function is always satisfied. The minimization problem for the first eigenvalue is a good play to start a description of the algorithm. The task is to find

$$\min_{\rho(x)} \lambda_1 = \min_{\rho(x)} \min_{v \in H_{(0)}^1} \frac{\int_D |\nabla v|^2 dx + \beta \int_{\partial D} v^2(x) dx}{\int_D \rho(x) v(x)^2 dx}.$$

Assume the eigenfunctions are normalized by $\int_D \rho(x) v(x)^2 dx = 1$. At iteration step i, there is a guess for the configuration density function ρ^i. Use the forward problem solver described in the previous section to find the corresponding eigenvalue $\lambda_1(\rho^i)$ and eigenfunction $u_1(\rho^i)$. For simplicity, denote them the eigenpair $(\lambda_{1,i}, u_{1,i})$. Thus

$$\lambda_{1,i} = \frac{\int_D |\nabla u_{1,i}|^2 dx + \beta \int_{\partial D} u_{1,i}^2(x) dx}{\int_D \rho^i u_{1,i}(x)^2 dx}.$$

Our goal is to find a density function $\rho(x)$ so that it can maximize the integral of the form

$$\int_D \rho u_{1,i}^2 dx. \tag{6}$$

Suppose ρ^{i+1} is a new guess, such that

$$\int_D \rho^{i+1} u_{1,i}^2 dx \geq \int_D \rho^i u_{1,i}^2 dx.$$

Then, a new estimate for $\lambda_{1,i+1}$ will be smaller since

$$\begin{aligned}\lambda_{1,i+1} &= \min_{v\in H_0^1} \frac{\int_D |\nabla v|^2 dx + \beta \int_{\partial D} v^2(x) dx}{\int_D \rho^{i+1}(x) v(x)^2 dx} = \frac{\int_D |\nabla u_{1,i+1}|^2 dx + \beta \int_{\partial D} u_{1,i+1}^2(x) dx}{\int_D \rho^{i+1} u_{1,i+1}(x)^2 dx} \\ &\leq \frac{\int_D |\nabla u_{1,i}|^2 dx + \beta \int_{\partial D} u_{1,i}^2(x) dx}{\int_D \rho^{i+1} u_{1,i}(x)^2 dx} \leq \frac{\int_D |\nabla u_{1,i}|^2 dx + \beta \int_{\partial D} u_{1,i}^2(x) dx}{\int_D \rho^i u_{1,i}(x)^2 dx} = \lambda_{1,i}. \end{aligned} \tag{7}$$

Therefore, the monotone decreasing sequence $\{\lambda_{1,i}\}$ determined by (7) must converge since it has a lower bound. The success of the procedure (7) depends on whether we can find a density function so that it maximizes an integral of the form (6).

Assume N is the total number of nodal points and d_j is the density function evaluated at each grid point P_j, that is, $d_j = \rho(P_j)$. Representing the density function as

$$\rho \approx \sum_{j=1}^N d_j \xi_j,$$

the integral (6) becomes

$$\int_D \rho u_{1,i}^2 dx = \sum_{j=1}^N d_j \int_D \xi_j u_{1,i}^2 dx = \sum_{i=1}^N d_j \psi_j,$$

where $\psi_j = \int_D \xi_j u_{1,i}^2 dx$. Similarly, a discrete approximation to the fixed weight constraint (3) is

$$\sum_{j=1}^N d_j \Xi_j = W, \quad \text{where } \Xi_j = \int_D \xi_j dx. \tag{8}$$

Thus, in the discrete level, (6) can now be stated as

$$\max_{d=(d_1,\ldots,d_N)} \sum_{j=1}^N d_j \psi_j, \tag{9}$$

subjects to constraints (8) and $d_j \in \{\rho_1, \rho_2\}$. (Note that the representation here may vary with respect to different finite element basis functions used.) This problem can be solved by using the following rearrangement inequality:

Rearrangement Inequality [25]. Let

$$a_1 \leq a_2 \leq \cdots \leq a_n \quad \text{and} \quad b_1 \leq b_2 \leq \cdots \leq b_n$$

be ordered sequences of real numbers. The inequality

$$a_n b_1 + \cdots + a_1 b_n \le a_{\sigma(1)} b_1 + a_{\sigma(2)} b_2 + \cdots + a_{\sigma(n)} b_n \le a_1 b_1 + a_2 b_2 + \cdots + a_n b_n$$

holds for every choice of permutation

$$a_{\sigma(1)}, \ldots, a_{\sigma(n)}$$

of $a_1, \ldots, a_n$.

This rearrangement inequality indicates that we should arrange d_j in the same order of ψ_j in order to achieve maximum. Physically, it means to place higher density material in the regions that the displacement is large. Notice that the density function values d_j is binary and (8) can be written

$$\rho_1 \sum_{\{j:d_j=\rho_1\}} \Xi_j + \rho_2 \sum_{\{j:d_j=\rho_2\}} \Xi_j = \rho_1\big(|D| - |\Omega|\big) + \rho_2\big(|\Omega|\big) = W. \tag{10}$$

This leads directly to the statement

$$|\Omega| = \frac{W - \rho_1 |D|}{\rho_2 - \rho_1}$$

which is the criterion for determining the threshold of the density function.

Remark 1 The rearrangement method we just described is essentially an alternating minimization with respect to ρ (rearrangement) and u (Rayleight principle). The efficiency of the algorithm is mainly due to the exact solution of the problem with respect to ρ for a fixed u.

Remark 2 In our numerical computation on a triangular mesh, we interpolate the values from the vertices to the value on the centroid in each triangle. In particular, a uniform triangular mesh is used to reduce possible effects from meshes. This is because the areas of triangular elements affect the sorting. If a uniform mesh is used in the numerical implementation, Ξ_j's are mostly the same for every j and $\Xi_j \approx \frac{|D|}{N}$. Thus, the threshold for distinguishing ρ_1 and ρ_2 will be at index

$$j^* = \frac{|D| - |\Omega|}{\Xi_j} = \frac{(\rho_2|D| - W)/(\rho_2 - \rho_1)}{|D|/N}, \tag{11}$$

and the density is assigned as

$$\rho_1 = d_1 = \cdots = d_{j*} < d_{j^*+1} = \cdots = d_N = \rho_2. \tag{12}$$

Notice that in this setting, only the square value $(u_{1,i}^j)^2$ are used for sorting ψ_j. We summarize the algorithm for fully sorting algorithm in Algorithm 1.

Remark 3 This fully sorting algorithm can be directly applied to solve simple λ_k for $k \ge 2$. Since there is a possibility that the k-th eigenvalue collides with its lower eigenvalues (($k-1$)-th eigenvalue or more), multiple eigenfunctions need to be considered while updating density distribution. We will address this in Sect. 3.6.

Algorithm 1 Fully sorting algorithm for minimization

initial guess for $\rho(x)$
do while not optimal

1. solve the elliptic eigenvalue problem (1) by the forward finite element method
2. sort ψ_j in the ascending order and compute the threshold index j^* as defined by (11)
3. update $\rho(x)$ by the process (12)

3.3 The Maximization of λ_k

The maximization problem becomes much more complicated since we have to deal with the *maxmin* case instead of *minmin* case. For the optimization problem

$$\max_{\rho(x)} \lambda_1 = \max_{\rho(x)} \min_{v \in H^1_{(0)}} \frac{\int_D |\nabla v|^2 dx + \beta \int_{\partial D} v^2(x) dx}{\int_D \rho(x) v(x)^2 dx}.$$

At the iteration step i, we seek the density function ρ^{i+1}, such that

$$\int_D \rho^{i+1} u_{1,i}^2 dx \le \int_D \rho^i u_{1,i}^2 dx. \tag{13}$$

In this way, we have

$$\lambda_{1,i+1} = \frac{\int_D |\nabla u_{1,i+1}|^2 dx + \beta \int_D u_{1,i+1}^2(x) dx}{\int_D \rho^{i+1} u_{1,i+1}(x)^2 dx} \le \frac{\int_D |\nabla u_{1,i}|^2 dx + \beta \int_D u_{1,i}^2(x) dx}{\int_D \rho^{i+1} u_{1,i}(x)^2 dx}, \tag{14}$$

and

$$\lambda_{1,i} = \frac{\int_D |\nabla u_{1,i}|^2 dx + \beta \int_D u_{1,i}^2(x) dx}{\int_D \rho^{i} u_{1,i}(x)^2 dx} \le \frac{\int_D |\nabla u_{1,i}|^2 dx + \beta \int_D u_{1,i}^2(x) dx}{\int_D \rho^{i+1} u_{1,i}(x)^2 dx}. \tag{15}$$

However, unlike the monotone property established in (7), the inequalities (14) and (15) do not guarantee a monotone increasing sequence and we need to add an acceptance- rejection step. After updating the density function, we will run the forward eigenvalue solver to check if the new configuration actually increases the eigenvalue. If the eigenvalue is increasing, the new configuration of the density function will be accepted. Otherwise, we will use Partial Swapping Method which will be introduced in Sect. 3.5.

In the discrete setting, the criterion (13) corresponds to arrange d_j is the reversed order of ψ_j in order to achieve the minimum. (See *Rearrangement Inequality*). This suggests that we should update the density function by placing lower density material at the locations with large ψ values and vice versa. Adopting the definition of threshold index j^* in (11), the updating process of the density function can be formulated as

$$\rho_2 = d_1 = \cdots = d_{N-j^*} > d_{N-j^*+1} = \cdots = d_N = \rho_1. \tag{16}$$

The sorting method as discussed above can be easily generalized to higher eigemodes by replacing the first eigenvalue λ_1 and its eigenfunction u_1 by the k-th eigenvalue λ_k and the corresponding eigenfunction u_k. We summarize the maximum algorithm in Algorithm 2.

Algorithm 2 Sorting maximization

initial guess for $\rho(x)$
solve the elliptic eigenvalue problem (1) by the forward finite element method
do while not optimal

1. sort ψ_j in the ascending order and compute the threshold index j^* as defined by (11)
2. update $\rho(x)$ by the process (16)
3. solve the elliptic eigenvalue problem (1) using the updated $\rho(x)$

- if the eigenvalue increases, accept $\rho(x)$
- if not, use Partial Swapping Method to generate a new $\rho(x)$

3.4 The Maximization of $\lambda_{k_2}/\lambda_{k_1}$

The third type of optimization problem we are interested in is

$$\max_{\rho(x)} \frac{\lambda_{k_2}}{\lambda_{k_1}} = \max \frac{\min\limits_{\substack{v\in H^1_{(0)}(\Omega)\\ v \text{ orthogonal to } u_1,u_2,\ldots,u_{k_2-1}}} \frac{\int_D |\nabla v|^2 dx+\beta\int_{\partial D} v^2(x)dx}{\int_D \rho(x)v(x)^2 dx}}{\min\limits_{\substack{v\in H^1_{(0)}(\Omega)\\ v \text{ orthogonal to } u_1,u_2,\ldots,u_{k_1-1}}} \frac{\int_D |\nabla v|^2 dx+\beta\int_{\partial D} v^2(x)dx}{\int_D \rho(x)v(x)^2 dx}}.$$

Different from the minimization or maximization problems of λ_k, at each iteration i, we need to consider the ratio

$$\frac{\lambda_{k_2}}{\lambda_{k_1}} = \frac{\frac{\int_D |\nabla u_{k_2}|^2 dx+\beta\int_{\partial D} u^2_{k_2}(x)dx}{\int_D \rho(x)u^2_{k_2}dx}}{\frac{\int_D |\nabla u_{k_1}|^2 dx+\beta\int_{\partial D} u^2_{k_1}(x)dx}{\int_D \rho(x)u^2_{k_1}dx}} = \frac{\int_D |\nabla u_{k_2}|^2 dx+\beta\int_{\partial D} u^2_{k_2}(x)dx}{\int_D |\nabla u_{k_1}|^2 dx+\beta\int_{\partial D} u^2_{k_1}(x)dx} \cdot \frac{\int_D \rho(x)u^2_{k_1}dx}{\int_D \rho(x)u^2_{k_2}dx}. \quad (17)$$

Notice that in (17) only the second ratio contains the density function $\rho(x)$. In term of discrete computation, the same argument for the integral (6) still applies here. Considering the numerator and the denominator of the second ratio in (17) separately, we have a linear fractional problem

$$\max_{d=(d_1,d_2,\ldots,d_N)} \frac{\sum_{j=1}^N d_j \psi_j^{k_1}}{\sum_{j=1}^N d_j \psi_j^{k_2}}, \quad \text{where } \psi_j^{k_{1(2)}} = \int_D \xi_j u^2_{k_{1(2)},i}dx. \quad (18)$$

subject to the constraints (8) and $d_j \in \{\rho_1, \rho_2\}$.

Here, we introduce Dinkelbach's iterative algorithm to solve this linear fractional programing problem ([3]). Dinkelbach's algorithm is based on the simple theorem: The vector x^* is an optimal solution of problem

$$\max_{x\in S} \frac{P(x)}{Q(x)} \quad (19)$$

where $P(x)$, $Q(x) \geq 0$ are linear functions of x, and S is the feasible set of the optimization problem if and only if

$$\max_{x\in S}\{P(x) - t^* Q(x)\} = 0 \quad \text{where } t^* = \frac{P(x^*)}{Q(x^*)}.$$

The Dinkelbach's iterative method to find an optimal solution is summarized in Algorithm 3.

Algorithm 3 Dinkelbach's Algorithm

initial guess for $x^{(0)} \in s$, calculate $t^{(1)} := \frac{P(x^{(0)})}{Q(x^{(0)})}$, set $m = 1$
do while $F(t^{(m)}) \neq 0$

1. $x^{(m)} := \operatorname{argmax}_{x \in S}\{P(x) - t^{(m)} Q(x)\}$
2. $t^{(m+1)} := P(x^{(m)})/Q(x^{(m)})$, set $m = m + 1$.

Noting that, when the algorithm is applied to solve (18), the step for solving

$$\operatorname*{argmax}_{x \in S}\left\{P(x) - t^{(m)} Q(x)\right\} = \operatorname*{argmax}_{d=(d_1,d_2,\ldots,d_N)} \sum_{j=1}^{N} d_j \left\{\psi_j^{k_1} - t^{(m)} \psi_j^{k_2}\right\}$$

is in fact the optimization problem as described in (9), except that ψ_j is replaced with $\psi_j^{k_1} - t^{(m)} \psi_j^{k_2}$. The sorting procedure and updating procedure (12) can be applied immediately to obtain the optimal configuration. Since this problem is of $maxmin$ type too, partial swapping algorithm will be adopted when the ratio is not increasing. Finally we summarize the method for maximizing the ratio of adjacent eigenvalues in Algorithm 4.

Algorithm 4 Algorithm for Maximization the ratio of adjacent eigenvalues

initial guess for $\rho(x)$
solve the elliptic eigenvalue problem (1) by the forward finite element method
do while not optimal

1. update $\rho(x)$ by solvig (18) via Dinkelbach's algorithm
2. solve the elliptic eigenvalue problem (1) using the updated $\rho(x)$
   - if the ratio of eigenvalues increases, accept $\rho(x)$.
   - if not, use Partial Swapping Method to generate a new $\rho(x)$ via Dinkelbach's algorithm

3.5 Partial Swapping Algorithm

As we can see from (15), the monotonicity is not guaranteed. When a configuration of the density function through fully sorting method does not increase the eigenvalue or the ratio of eigenvalues, the partial swapping method will be used. Figure 1 illustrates this method. Let set A (within the red circle) be the current configuration of the density function with value ρ_1, and set B (within the blue circle) be the suggested configuration with density value ρ_1 which is obtained from fully sorting method. Left panel in Fig. 1 explains the fully sorting method. If the suggested configuration increases the target eigenvalue we will accept it, that is, switch the density values in the difference set $A \backslash B$ (light gray region) and $B \backslash A$ (dark gray region). However, if this configuration fails, we choose subsets of $A \backslash B$ and $B \backslash A$, say sets C(light gray region) and D (dark gray region) as labeled in Fig. 1 (right panel), and switch their density values. Subsets C and D are of the same size in order to satisfy the fixed

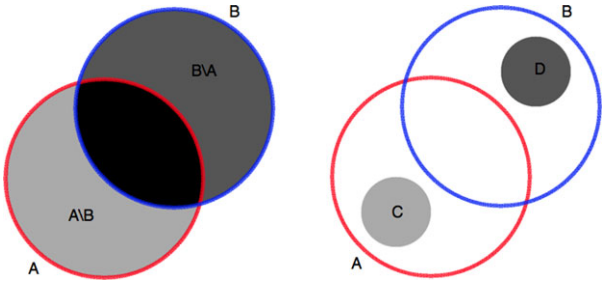

Fig. 1 An illustration of partial swapping method. *Left panel* shows the fully sorting method switch the density values in the difference set $A\backslash B$ (*light gray region*) and $B\backslash A$ (*dark gray region*). *Right panel* shows the partial swapping method: switch the density values in the subsets C (*light gray region*) and D (*dark gray region*)

weight assumption. The size of the subsets is a parameter which can be adjusted. For example, $|C| = \mu|A\backslash B|$ and $|D| = \mu|B\backslash A|$ where $\mu \in (0, 1)$. Due to the numerical discretization, we will choose $\mu \in (\epsilon, 1)$ where ϵ is the area ratio of one element and the whole domain in order to avoid the possibility of empty set in C or D. In our numerical implementation, we kept halving the size until we reach a density configuration which increases the target eigenvalue. We follow the sorting idea in selecting the subsets C and D. Take $\max_{\rho(x)} \lambda_1$ for example, at iteration step i, if the fully sorting method fails, subset C in $A\backslash B$ of prescribed size is generated according to sorting ψ_j which is a constant multiple of the squared eigenfunction values in this case, preferring small values. Contrary to subset C, large squared eigenfunction values are preferred for subset D. Finally, we switch the density values in C and D instead of $A\backslash B$ and $B\backslash A$. This kind of swapping method can easily generate topological changes. This partial swapping technique is summarized in Algorithm 5. Notice that there are many different ways to do partial swapping algorithm as long as the swapping sets are chosen differently. Another possible partial swapping algorithm is to swap the density values near the interface of two densities in the previous iteration. This approach is similar to the idea of shape derivatives which consider the local variation of density near the interface.

3.6 Gradient at Eigenvalues with Multiplicity Greater than One

Here we discuss the strategy for an eigenvalue with multiplicity. The generalized gradient is considered, as the classical derivative does not exit in this case. In the work of S. Cox [9], the strategy for computing the generalized gradient of the extreme eigenvalues has been explained and applied to an elliptic operator. Here we summarize the fundamental results. Recall that the generalized directional derivative of a Lipschitz function $\mathcal{F}$ on the Banach space X at f in the direction of g is

$$\mathcal{F}^0(f; g) = \lim \sup_{\substack{h \to f \\ t \downarrow 0}} \frac{\mathcal{F}(h + tg) - \mathcal{F}(h)}{t}.$$

The generalized gradient of F at f is defined by the nonempty, convex, weak* compact set

$$\partial F(f) \equiv \left\{\xi \in X'; \mathcal{F}^0(f; g) \geq \{\xi, g\}_X \ \forall g \in X\right\},$$

where X' denotes the dual space of X. For the elliptic eigenvalue problem (1), we assume an eigenvalue with multiplicity m when $\rho = \rho_0$:

$$\lambda_{k-1}(\rho_0) < \lambda_k(\rho_0) = \cdots = \lambda_{k+m-1}(\rho_0) < \lambda_{k+m}(\rho_0), \quad m > 1.$$

Then

$$\partial\lambda_k(\rho_0) = \partial\lambda_{k+m-1}(\rho_0) = \operatorname{co}\left\{-\lambda u^2 : u \in \varepsilon_k^1(\rho_0)\right\}, \tag{20}$$

Algorithm 5 Partial swapping algorithm

Let set A (within the red circle in Fig. 1) be the current configuration of the density function with value ρ_1 and set B (within the blue circle in Fig. 1) be the suggested configuration with density value ρ_1 which is obtained from fully sorting method.
Find the difference sets $A\backslash B$ and $B\backslash A$.
Choose a constant $\mu \in (\epsilon, 1)$ (In our implementation, $\mu = \frac{1}{2}$ and ϵ is the area ratio of one element and the whole domain)
do while the objective function is not increasing and $\mu > \epsilon$

1. choose subset C in $A\backslash B$ which corresponds to smaller square value of ψ_j such that $|C| = \mu|A\backslash B|$
2. choose subset D in $B\backslash A$ which corresponds to larger square value of ψ_j such that $|D| = \mu|B\backslash A|$
3. swap the density in C and D, i.e. $\rho(x) = \rho_2$ in C and $\rho(x) = \rho_1$ in D

   - if the objective function increases, accept $\rho(x)$ and terminate the partial swapping algorithm
   - if not, reduce μ by half

where co is the convex hull and $\varepsilon_k^1(\rho)$ is the span of all eigenfunctions u corresponding to the eigenvalue λ_k with the normalization $\int_D \rho_0 u^2 dx = 1$. Utilizing the idea in (20), we use the generalized gradient direction at an eigenvalue with multiplicity m while maximizing of eigenvalue is performed,

$$-\operatorname{co}\left(u_j^2\right), \quad j = k, \ldots, k+m-1,$$

where u_j is the j-th eigenfunction. For example, for eigenvalues with multiplicity 2, i.e. $\lambda_k(\rho_0) = \lambda_{k+1}(\rho_0)$, then the linear combination

$$\alpha u_k^2 + (1-\alpha)u_{k+1}^2, \quad 0 < \alpha < 1,$$

is used as the reference function for sorting. In general, a $(m-1)$-dimensional optimization problem need to be solved. In the numerical simulation, we will show an example that the right direction in searching for maximization of λ_2 in a square domain is

$$\frac{1}{2}u_k^2 + \frac{1}{2}u_{k+1}^2. \tag{21}$$

4 Numerical Simulation

We first consider solving the optimization problem on a rectangular domain $\Omega = [0,1] \times [0,1.5]$ described in [19]. We use finite element method with a triangular mesh on Ω to solve the forward eigenvalue problem. Initially we divide the rectangular into 8 triangles as shown in Fig. 2(a) and then refine the mesh in the standard way by subdividing each triangles into four triangles as shown in Fig. 2(b). The numerical results are done on the 7-th refinement which gives $8 \times 4^7 = 131072$ triangles. The initial density distribution is chosen as

$$\rho = \begin{cases} \rho_1 = 1 & \text{if } |x - 0.75| \geq 0.375, \\ \rho_2 = 2 & \text{if } |x - 0.75| < 0.375 \end{cases} \tag{22}$$

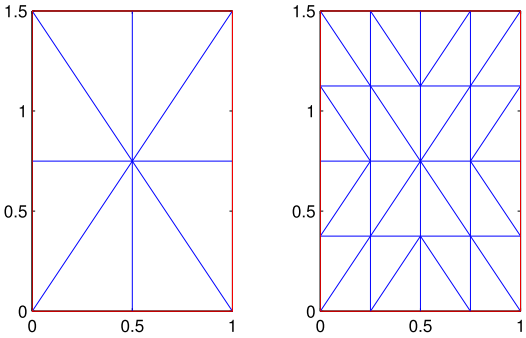

Fig. 2 (**a**) The initial mesh. (**b**) The first refinement

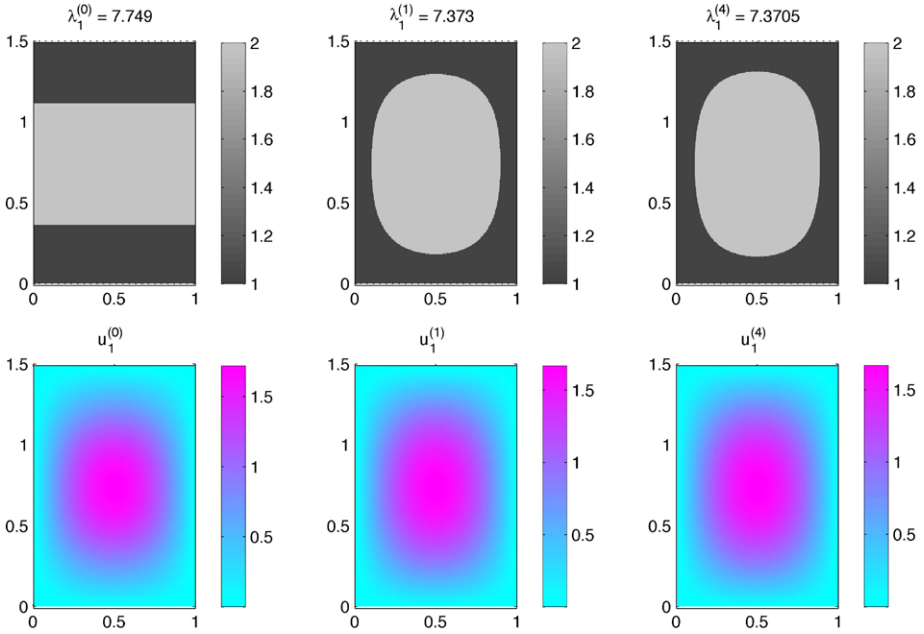

Fig. 3 The evolution of density distributions is shown in the first row for minimization of the first eigenvalue with Dirichlet boundary condition at 0, 1st, and 4th iterations. The corresponding eigenfunctions are shown in the second row at 0, 1st, and 4th iterations

with $W = 2.25$. The numerical accuracy of eigenvalues is of second order. The same stopping criterion is used for all the simulations. That is, when the difference between eigenvalues in two consecutive iterations is less than 10^{-6}.

In Fig. 3, we show the evolution of density distribution for zero, first, and fourth iteration for minimization of the first eigenvalue λ_1 with Dirichlet boundary condition in the first row. The corresponding eigenfunctions for zero, first, and fourth iteration are shown in the second row respectively. It only takes four iterations in total while the method based on shape derivative requires hundred of iterations to reach the minimum [19]. We see that the proposed method gives a very good rearrangement of density distribution in the first iteration. The corresponding eigenvalue evolution is shown in Fig. 4. Furthermore, the number of iteration stays roughly the same while different sizes of meshes are used.

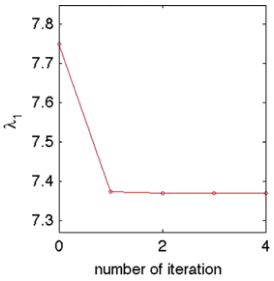

Fig. 4 The evolution of eigenvalue for the minimization of the first eigenvalue with Dirichlet boundary condition

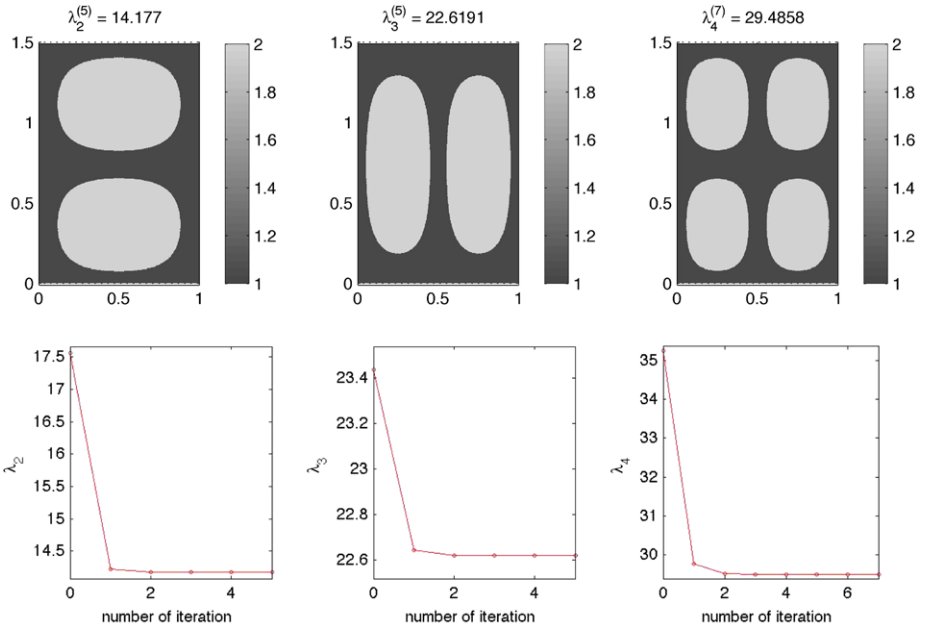

Fig. 5 The density distributions for minimization of the second, third, fourth eigenvalues with Dirichlet boundary condition are shown in the *first row* respectively. The corresponding eigenvalue evolutions are shown in the *second row*

With the same initial guess (22), we minimize λ_2, λ_3, and λ_4 with Dirichlet boundary condition and show the numerical optimized density distribution in the first row in Fig. 5. The corresponding eigenvalue evolutions are shown in the second row in Fig. 5. The optimized density distributions have symmetric structure. If the domain is divided by the nodal lines where the eigenfunction is zero, the density distributions have two-, two-, four-fold symmetry as shown in the second row in Fig. 4. We remark here that the rearrangement algorithm does not guarantee the global minimization. In this numerical test, the optimized density distribution for λ_4 is a local minimizer (not the global minimizer). We repeated the numerical simulations with many different initial guesses of density distribution and found a smaller optimized density distribution for λ_4. The density distribution is shown at the initial, first and second iterations in Fig. 6. For the first to third eigenvalues, the optimal results turn out to be the same for all different initial conditions we have tried. This tells us that high eigenmodes are probably more nonconvex in terms of density distribution.

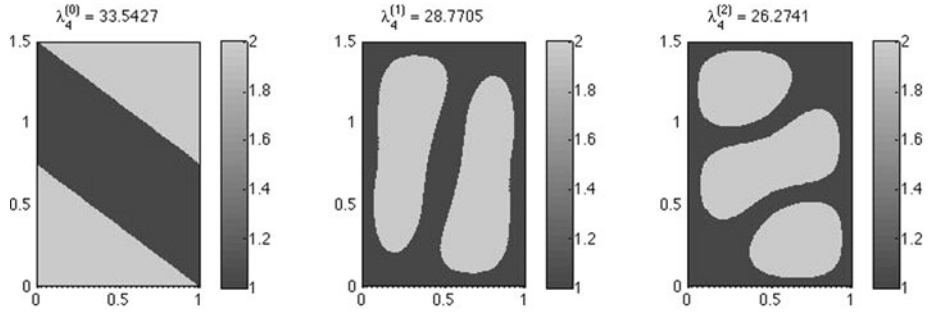

Fig. 6 The density distributions at the initial, 1st, and 2nd iterations for minimization of fourth eigenvalue with Dirichlet boundary condition

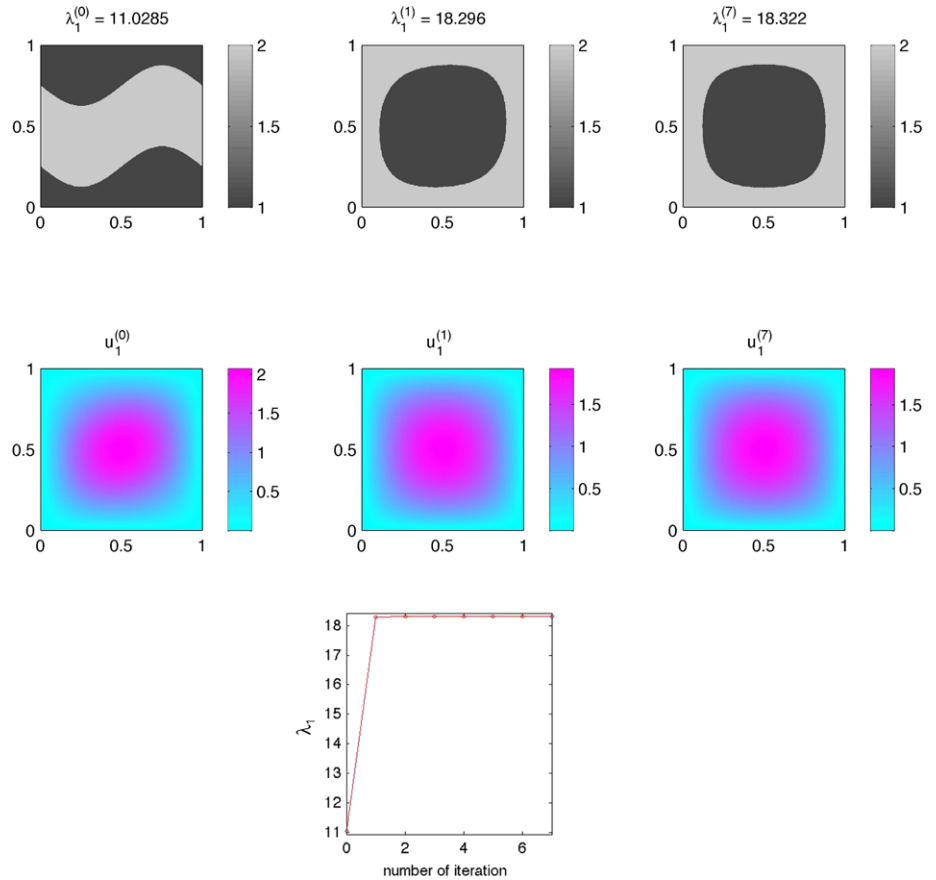

Fig. 7 The evolution of density distributions is shown in the *first row* for maximization of the first eigenvalue with Dirichlet boundary condition at 0, 1st, and 7th iterations. The corresponding eigenfunctions are shown in the *second row* at 0, 1st, and 7th iterations. The evolution of corresponding eigenvalues is shown in the *third row*

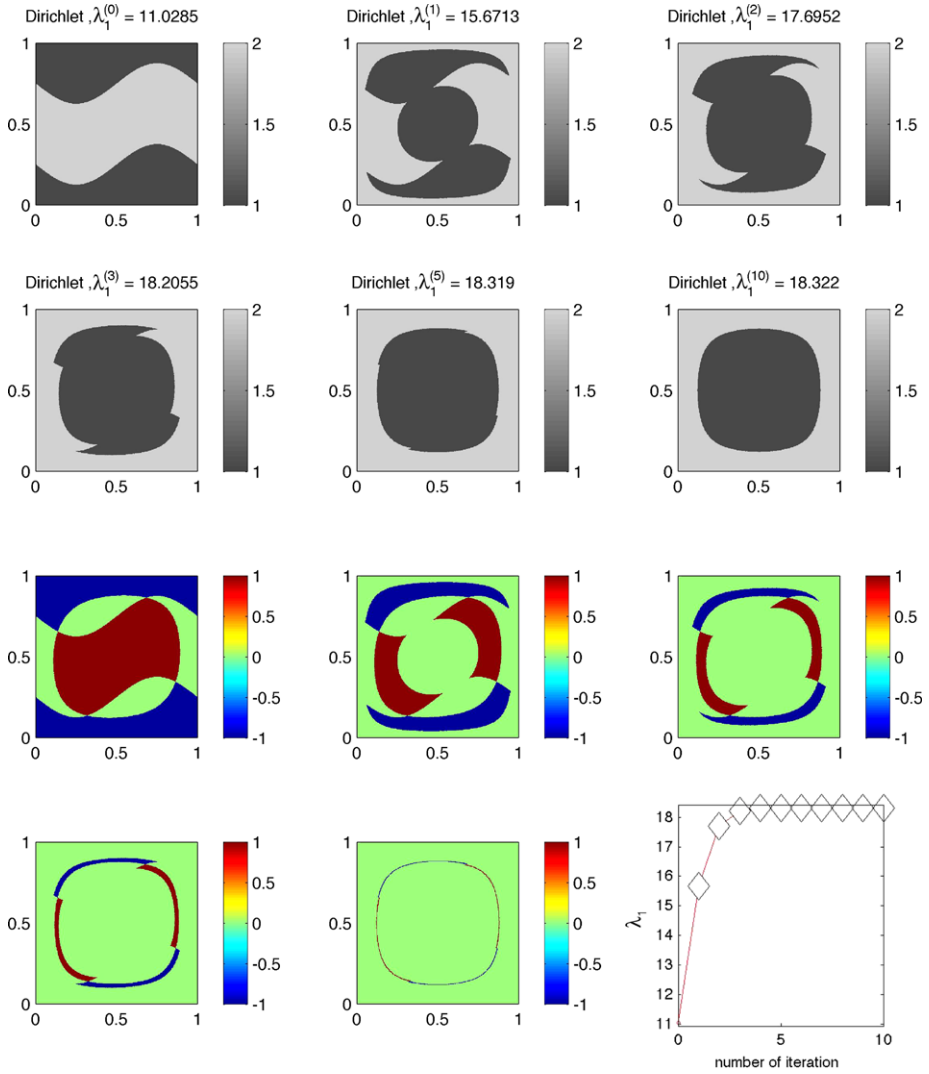

Fig. 8 The evolution of density distributions is shown in the *first and second rows* for maximization of the first eigenvalue with Dirichlet boundary condition at 0, 1st, 2nd, 3th, 5th and 10th iterations. The partial swapping method with half of the difference set is applied at each iteration. In the *third and fourth rows*, we show the difference sets at 0, 1st, 2nd, 3th and 5th. The *blue region* indicates the set $A \setminus B$ while the *red region* indicates the set $B \setminus A$. The evolution of corresponding eigenvalues is shown in the last figure in the *fourth row*

For maximization of eigenvalue problems, we demonstrate the results on the square domain $\Omega = [0, 1] \times [0, 1]$ because multiplicity can occur more frequently. Figure 7 shows the results for $\max_\rho \lambda_1$ with Dirichlet boundary condition. The calculations start with an initial guess of a trigonometric wave shape containing density value ρ_2, as shown for $\lambda_1^{(0)}$. Subsequent results for iterations 1 ($\lambda_1^{(1)}$) and 7 ($\lambda_1^{(7)}$), indicate the approach to the maximum. The "optimal" result ($\lambda_1^{(7)}$) shows that the places with larger density value ρ_2 are attached to

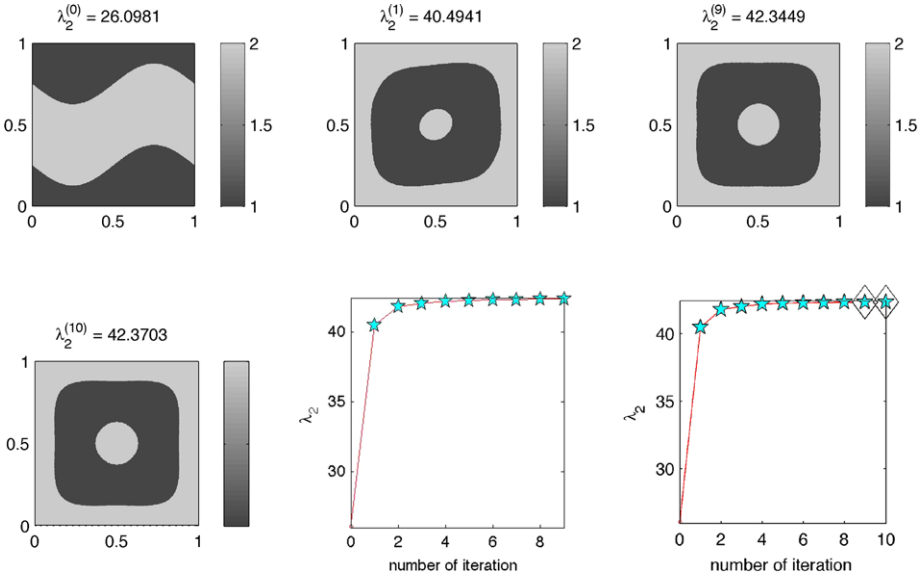

Fig. 9 The evolution of density distribution is shown in the *first row* for maximization of the second eigenvalue at 0, 1st and 9th iterations without partial rearrangement. The evolution of density distribution at 10th iteration with partial rearrangement. We can see that partial rearrangement algorithm provides larger λ_2. The evolutions of corresponding eigenvalues are shown in the *center and right figures in the second row* for the simulations without and with partial rearrangement, respectively. A *filled star* is marked if the generalized gradient (21) is applied while a *diamond shape* is marked when partial rearrangement is applied

the boundary. The third row in Fig. 7 plots the changes in λ_1. The maximal value of λ_1 is 18.322.

In Fig. 8, we demonstrate that the partial swapping method can also be applied to find the maximization of λ_1. Here the swapping sets C and D are half size of different sets $A \setminus B$ and $B \setminus A$ mentioned in Sect. 3.5. The evolution of density distributions is shown in the first and second rows for maximization of the first eigenvalue with Dirichlet boundary condition at 0, 1st, 2nd, 3th, 5th, and 10th iterations. In the third and fourth rows, we show the difference sets at 0, 1st, 2nd, 3th and 5th. The blue region indicates the set $A \setminus B$ while the red region indicates the set $B \setminus A$. The evolution of corresponding eigenvalues is shown in the last figure in the fourth row. A diamond is marked at the third iteration when the partial swapping method is applied. We see that the topology can be changed easily during the evolution. At the end, the optimal value of $\max \lambda_1$ is the same as the result in the previous example. Notice that the iteration number increases when the partial swapping method is used. When a smaller size of swapping region is used, the more number of iterations is needed to converge.

Figure 9 shows the results for $\max_\rho \lambda_2$. We perform simulations without and with partial rearrangement algorithm in order to see whether partial rearrangement improve the optimization results in some cases. The calculations start with the same initial guess of a trigonometric wave shape containing density value ρ_2, as shown for $\lambda_1^{(0)}$. The subsequent results are shown for iterations 1 ($\lambda_2^{(1)}$) and 9 ($\lambda_2^{(9)}$) for fully rearrangement algorithm and 10 ($\lambda_2^{(10)}$) for partial rearrangement algorithm. The "optimal" results show that the places with smaller density value ρ_1 looks like a square washer. We can see that partial rearrangement algorithm provides larger λ_2. The evolutions of corresponding eigenvalues are shown in the

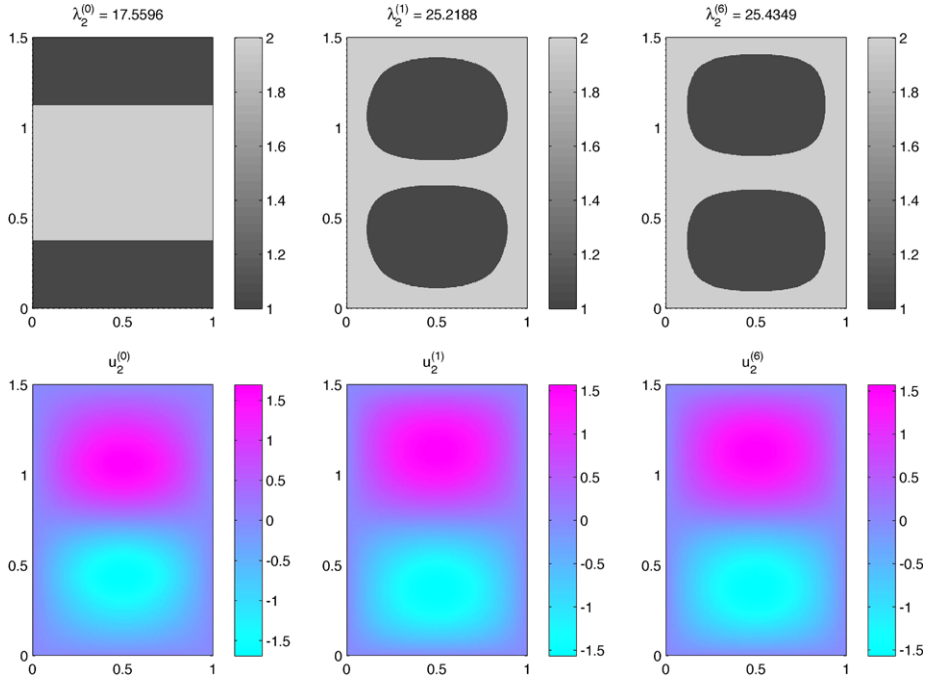

Fig. 10 The evolution of density distributions is shown in the *first row* for maximization of the second eigenvalue with Dirichlet boundary condition at 0, 1st, and 6th iterations. The corresponding eigenfunctions are shown in the *second row* at 0, 1st, and 6th iterations

center and right figures in the second row for the simulations without and with partial rearrangement, respectively. A filled star is marked if the generalized gradient (21) is applied while a diamond shape is marked when partial rearrangement is applied. While we optimize the second eigenvalue λ_2, λ_2 and λ_3 collide with each other. Thus, the generalized gradient idea (21) applies here. A linear combination $\frac{1}{2}(u_2^2 + u_3^2)$ is used in the sorting process at each step, where u_2 and u_3 are the corresponding eigenfunctions.

Figure 10 shows the results for $\max_\rho \lambda_2$ on the rectangular domain. The calculations start with the same initial guess of a strip containing density value ρ_2 as the example in Fig. 3. The "optimal" result ($\lambda_2^{(6)}$) has the reciprocal rearrangement of density for $\min \lambda_2$ shown in Fig. 5. Notice that this optimal density distribution is very different from the result on the square domain shown in Fig. 9 since the multiplicity does not occur in the rectangular domain.

We now investigate the role of the Robin boundary parameter β in the maximization problem $\max_\rho \lambda_3^R$. Figure 11 shows the optimal results for $\beta = \infty, 10, 1, 0$. As $\beta \to \infty$, the Robin boundary condition asymptotes to the Dirichlet boundary condition, shown as the first graph in Fig. 11. As $\beta \to 0$, the Robin boundary condition becomes the Neumann boundary condition, shown as the last graph in the sequence. There is a gradual change as the two triangle shaped regions with density ρ_1 are pushed to the diagonal corners and then morph into two fan-like regions.

For the maximization of the ratio of adjacent eigenvalues, only the Dirichlet Boundary problems will be considered. Figure 12 shows the results for $\max_\rho \lambda_2/\lambda_1$. The calculations start with an initial guess of a strip containing density value ρ_2, as shown for $(\lambda_2/\lambda_1)^{(0)}$,

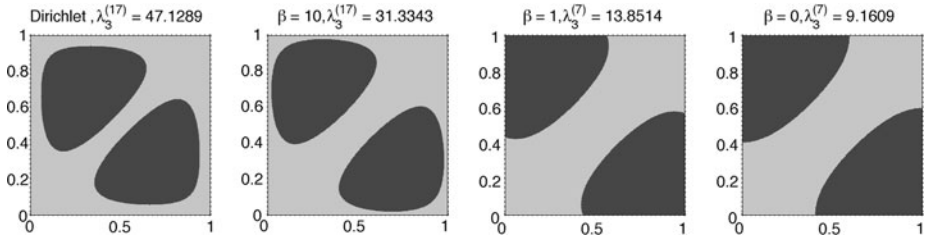

Fig. 11 The optimal results of $\max_\rho \lambda_3^R$ for $\beta = \infty, 10, 1, 0$

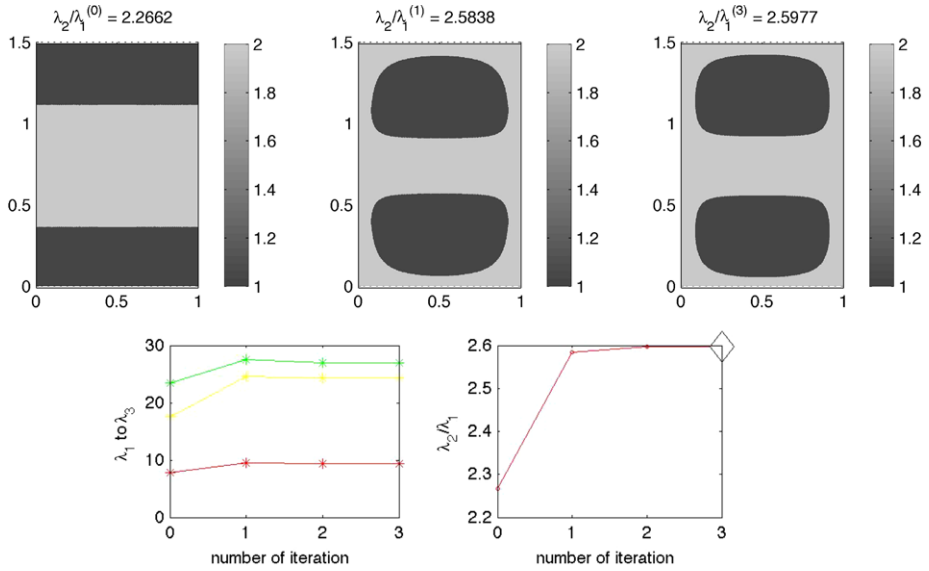

Fig. 12 The evolution of density distributions is shown in the *first row* for maximization of λ_2/λ_1. The evolutions of individual eigenvalue from λ_1 to λ_3 and the ratio λ_2/λ_1 are shown in the *second row*

and the subsequent results for iterations 1 $((\lambda_2/\lambda_1)^{(1)})$, 2 $((\lambda_2/\lambda_1)^{(2)})$, 3 $((\lambda_2/\lambda_1)^{(3)})$ show convergence. It takes 3 steps to converge. The second row in Fig. 12 plots the changes in the individual eigenvalue from λ_1 to λ_3 and in the ratio of eigenvalues λ_2/λ_1. The optimal density distribution is similar to the result of $\max \lambda_2$ shown in Fig. 10 but very different from the result of $\min \lambda_1$ shown in Fig. 3.

Figure 13 shows the results for $\max_\rho \lambda_3/\lambda_2$. The calculations start with an initial guess which is the same as the previous example and the subsequent results for iterations 2 $((\lambda_3/\lambda_2)^{(2)})$ and 6 $((\lambda_3/\lambda_2)^{(6)})$ are shown. It takes 6 steps to converge. The second row in Fig. 13 plots the changes in the individual eigenvalue from λ_1 to λ_4 and in the ratio of eigenvalues λ_3/λ_2. There is a degeneracy in λ_3, so a linear combination $\frac{1}{2}(u_3^2 + u_4^2)$ is used in the sorting process at each step, where u_{3-4} are the corresponding eigenfunctions. At the first few iterations, fully sorting method directly increases the ratio λ_3/λ_2. However, as the ratio keeps increasing, it becomes harder for the fully sorting method to directly increase the ratio. Thus the partial swapping is used at the fifth and sixth iterations and it fine-tunes the result to be optimal.

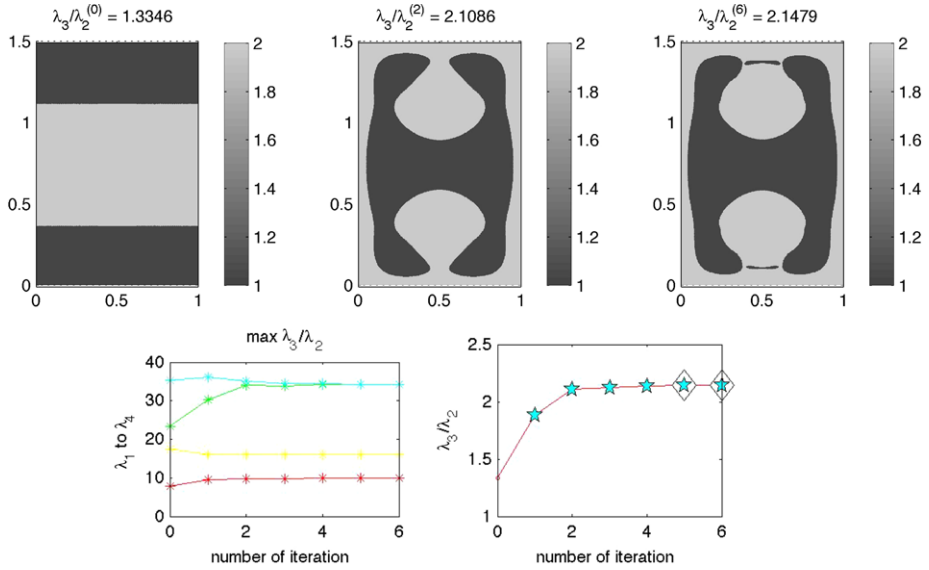

Fig. 13 The evolution of density distributions is shown in the *first row* for maximization of λ_3/λ_2. The evolutions of individual eigenvalue from λ_1 to λ_4 and the ratio λ_3/λ_2 are shown in the *second row*

From the above numerical results, we see that the rearrangement algorithms can efficiently optimize the eigenvalue problems: $\min \lambda_k$, $\max \lambda_k$, and $\max \lambda_{k_2}/\lambda_{k_1}$. The algorithms are much more efficient than the level set approaches based on shape derivative and/or topological derivative. Whether or not the rearrangement algorithms converge to the global extremum depends on the initial guess. For the first few eigenvalues, the algorithms are quite robust in finding the global extremum numerically. The theoretical investigation on the convergence of the algorithms and the convergence rate requires further study. In this paper, only simple domain geometry and objective functions are considered. We will investigate these general problems and report them in a future paper.

References

1. Allaire, G.: Shape Optimization by the Homogenization Method. Springer, New York (2001)
2. Amstutz, S., Andrä, H.: A new algorithm for topology optimization using a level-set method. J. Comput. Phys. **216**, 573–588 (2006)
3. Bajalinov, E.B.: Linear-Fractional Programming: Theory, Methods, Applications and Software. Kluwer Academic, Boston (2003)
4. Bendsoe, M., Sigmund, O.: Topology Optimization. Theory. Methods and Applications. Springer, New York (2003)
5. Burger, M.: A framework for the construction of level set methods for shape optimization and reconstruction. Inverse Probl. **17**, 1327–1356 (2001)
6. Burger, M., Hackl, B., Ring, W.: Incorporating topological derivatives into level set methods. J. Comput. Phys. **194**, 344–362 (2004)
7. Cox, S.: The two phase drum with the deepest bass note. Jpn. J. Ind. Appl. Math. **8**, 345–355 (1991)
8. Cox, S., McLaughlin, J.: Extremal eigenvalue problems for composite membranes I and II. Appl. Math. Optim. **22**, 153–167 (1990)
9. Cox, S.J.: The generalized gradient at a multiple eigenvalue. J. Funct. Anal. **133**, 30–40 (1995)
10. Haber, E.: A multilevel, level-set method for optimizing eigenvalues in shape design problems. J. Comput. Phys. **198**, 518–534 (2004)

11. He, L., Kao, C.-Y., Osher, S.: Incorporating topological derivatives into shape derivatives based level set methods. J. Comput. Phys. **225**, 891–909 (2007)
12. Henrot, A.: Extremum Problems for Eigenvalues of Elliptic Operators. Birkhäuser, Basel (2006)
13. Ito, K., Kunischm, K., Li, Z.: Level-set function approach to an inverse interface problem. Inverse Probl. **17**, 1225–1242 (2001)
14. Kao, C.-Y., Lou, Y., Yanagida, E.: Principal eigenvalue for an elliptic problem with indefinite weight on cylindrical domains. Math. Biosci. Eng. **5**, 315–335 (2008)
15. Kao, C.Y., Osher, S., Yablonovitch, E.: Maximizing band gaps in two dimensional photonic crystals by using level set methods. Appl. Phys. B, Lasers Opt. **81**, 235–244 (2005)
16. Kao, C.-Y., Santosa, F.: Maximization of the quality factor of an optical resonator. Wave Motion **45**(4), 412–427 (2008)
17. Krein, M.G.: On certain problems on the maximum and minimum of characteristic values and on the Lyapunov zones of stability. In: American Mathematical Society Translations, pp. 163–187 (1955)
18. Murqat, F., Simon, S.: Etudes de problems d'optimal design. Lect. Notes Comput. Sci. **41**, 52–62 (1976)
19. Osher, J., Santosa, F.: Level set methods for optimization problems involving geometry and constraints. I. Frequencies of a two-density inhomogeneous drum. J. Comput. Phys. **171**, 272–288 (2001)
20. Osher, S., Sethian, J.A.: Fronts propagating with curvature-dependent speed: algorithms based on Hamilton-Jacobi formulations. J. Comput. Phys. **79**(1), 12–49 (1988)
21. Rayleigh, J.W.S.: The Theory of Sound, vols. 1, 2. Dover, New York (1945)
22. Sethian, J., Wiegmann, A.: Structural boundary design via level set and immersed interface methods. J. Comput. Phys. **163**, 489–528 (2000)
23. Sokolowski, J., Zolesio, J.-P.: Introduction to Shape Optimization: Shape Sensitivity Analysis, vol. 10. Springer, Heidelberg (1992)
24. Su, S.: Numerical approaches on shape optimization of elliptic eigenvalue problems and shape study of human brains. PhD thesis, The Ohio State University (2010)
25. Wayne, A.: Inequalities and inversion of order. Scr. Math. **12**, 164–169 (1946)
26. Zhu, S., Wu, Q., Liu, C.: Variational piecewise constant level set methods for shape optimization of a two-density drum. J. Comput. Phys. **229**, 5062–5089 (2010)